

Full Length Research Paper

Induction of apoptosis and cell proliferation inhibition by paclitaxel in FM3A cell cultures

Nazlı N. Ilgar and Gül Özcan Arıcan*

Istanbul University, Faculty of Science, Department of Biology, Istanbul/Turkey.

Accepted 2 December, 2008

In this study, anti-proliferative and apoptotic effects of paclitaxel, which is itself an anti-chemotherapeutic agent, to FM3A cell line originated from Mouse mammary carcinoma at 7 different doses were examined. Seven different doses of paclitaxel (P1 = 3 nM, P2 = 7.5 nM, P3 = 15 nM, P4 = 30 nM, P5 = 60 nM, P6 = 120 nM, P7 = 240 nM) were administered to cells for 24 and 48 h. Growth rate measurements showed that living cell number decreased and number of dead cells increased ($p < 0.05$). Acquired growing rates were supported by mitochondrial dehydrogenase enzyme activity. Loss of volume, protrusions at plasma membrane (bleb formations), nuclear condensations and fragmentations, and apoptotic body formations were observed in cells whose morphologic criteria were examined by phase contrast and fluorescent microscope. According to apoptotic index rates determined by DAPI, most intense apoptotic cell formations were observed for P2 dose, which is accepted as critical for this cell line. DNA fragmentations were shown by agarose gel electrophoresis method. Acquired deductions showed that of the seven different doses of paclitaxel, P2 (7.5 nM) was the best dose to induce apoptosis in FM3A cells for 24 and 48 h.

Key words: *in vitro*, FM3A, cell kinetics, DNA, apoptosis, paclitaxel.

INTRODUCTION

Antimicrotubule agents have for many years been important anticancer agents, contributing significantly to the potentially curative treatment of diseases. Paclitaxel (PAC), extracted as early as the late 1960s from the bark of the Pacific Yew *Taxus brevifolia*, is the first compound with a taxane ring shown to possess antitumor activity (Moos and Fitzpatrick, 1998). Previous studies performed over the past 15 years have demonstrated that all the agents currently utilized to treat cancer can induce apoptosis in susceptible cell types *in vitro* and *in vivo* (Hu and Kavanagh, 2003). Understanding and evaluating the contribution of different forms of cell death to cancer development and treatment requires consideration of their individual mechanism of action and their genetic determinants. Killing malignant cells is the number one goal of almost all forms of cancer therapy in use today. In

the era of modern cancer therapy, researchers have developed innumerable ways to kill cancerous cells by triggering apoptosis, a genetically programmed form of cell suicide (Kim et al., 2002; Lockshin and Zakeri, 2004; Yi-ting et al., 2008).

For the purpose here, we discuss each of these anti-proliferative and apoptotic effects of PAC to FM3A cell line originated from Mouse mammary carcinoma at 7 different doses is examined. In this study, anti-proliferative and apoptotic effects of seven different doses of PAC which were applied for 24 and 48 h were investigated on FM3A cell lines. For this investigation, parameter of proliferation speed which shows PAC's anti-proliferative effects were determined with hemocytometer by counting living and dead cells. In addition, mitochondrial dehydrogenase enzyme activity of cells by WST-1 colorimetric assay kit of all experiment groups were detected to show surviving cells. In our experiments, we also used molecular biology methods and morphological imaging methods with apoptotic index (AI) parameters to assess PAC-induced apoptosis.

*Corresponding author. E-mail: gozcan@istanbul.edu.tr. Tel: 00 212 455 57 00 ext. 15093. Fax: 00 212 528 05 27.

MATERIALS AND METHODS

Cell culture

Tumor cell line used in our experiments was FM3A cells that was taken from mouse mammary cells. Cells were cultured in RPMI-1640 (Roswell Park Memorial Institute 1640, Sigma) containing 10% fetal bovine serum (FBS, Gibco Lab.) at 37°C in a humidified atmosphere of 5% CO₂ in air. Cells were washed with Hank's balanced salt solution (HBSS) and then centrifuged at 1500 rpm for 3 min. Supernatant was discarded and pellet was diluted with RPMI. Cells were seeded 30.000 cells/well in 96 well plates. After these, the cells were incubated at 37°C for 24 h.

Drug treatments

100 mg/16.6 ml PAC (Ebetaxel®, EBEWE Pharma., Unterach-Austria) were dissolved in RPMI as a 1 mg/ml stock solution supplemented with 10% FBS. The pH of the drug solution was adjusted to 7.4 with NaHCO₃. The experiments were tested by using P1 = 3 nM, P2 = 7.5 nM, P3 = 15 nM, P4 = 30 nM, P5 = 60 nM, P6 = 120 nM, P7 = 240 nM, doses were treated to FM3A cells in the time periods of 24 and 48 h.

Chemical

PAC consists of an eight-member taxane ring with a four-member oxetane ring and a bulky ester side chain at C-13 that is necessary for antitumor activity (Figure 1). The chemical formula of PAC is C₄₇H₅₁NO₁₄ and its molecular weight is 853.9 (Mastropaolo et al., 1995).

Hemocytometer assay

The growth rate of FM3A cells was determined with in 24 and 48 h. After these periods, the cells were selected in each well with 0.25 % trypsin. Both control and treatment groups were counted on hemocytometer with trypan blue under light microscope. Then growth rate was evaluated by counting viable and dead cells from each well.

WST-1 colorimetric assay

The effects of chemotherapeutic agents on the growth rates of FM3A cells were evaluated with the WST-1 assay kit (Premix WST-1, Takara, cat no: MK400). The WST-1 assay was applied to identify cytotoxicity that was formed by drug for 24 and 48 h. Therefore, WST-1 reagent; 4 h later, the 96 well plates were read on a Mquant Microelisa reader, using a test wavelength of 570 nm, a reference wavelength of 630 nm.

Apoptosis assay

For the determination of the AI, cells were fixed under methanol and stained with 4'-6-diamidine-2 phenylindole (DAPI). Following extensive washing in phosphate-buffered saline (PBS), slides were scored in double-blind under the fluorescence microscope. The AI represents the percentage of fragmented nuclei and was determined on a microscopic field of at least 100 area/each experimental points by the same scorer.

DNA fragmentations

Total DNA isolation was isolated from FM3A cells described in the

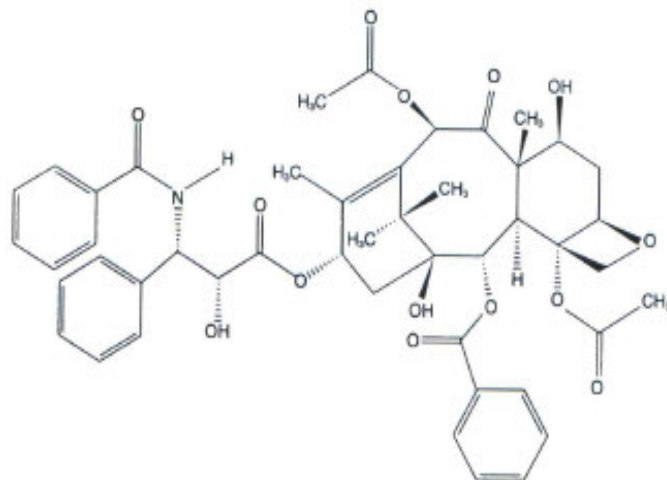


Figure 1. Chemical structure of PAC.

protocol of manufacturer (Apopladder Ex™ Kit, Takara, Cat. No. MK600). The DNA concentration of samples was measured with visible spectro photometer (GBC Cintra 20) at A₂₆₀ and electrophoresed in 2% (w/v) agarose containing 1 µg/ml ethidium bromide.

Statistical analysis

The data were analyzed statistically using ANOVA. Dunnett's test (between control and treatments groups) and Student Newman-Keuls test (between treatments groups) were used for multiple comparisons. The data analyzed were those from a minimum of three independent experiments. For the statistical evaluation of the results, the significance was accepted at the probability level of p < 0.05.

RESULTS

Growth inhibitory effect of paclitaxel

Hemocytometer results: Cytotoxic effects of seven different doses of PAC which were applied for 24 and 48 h were determined with hemocytometer by counting living and dead cells. Results of 24 and 48 h treatments of seven different doses of PAC to FM3A cells are showed on Figure 2. 30,000 cells of control group were counted to be 50,000 after 24 h cultivation. Statistically differences (p < 0.05) were found between experiment groups compared to the control group, except for P1 dose. In 48 h treatment groups, cells number of control became 112000 cells. All experiment groups for 48 h were statistically significant compared to control. Among groups of P1, P2, P3, P4, P5, P6 and P7, differences were not significant.

Vitality % graphic which was determined by counting living cells is showed on Figure 3. Comparing to the control group whose vitality was 100%, vitalities of experiment groups after 24 h were detected as 85% for P1 dose,

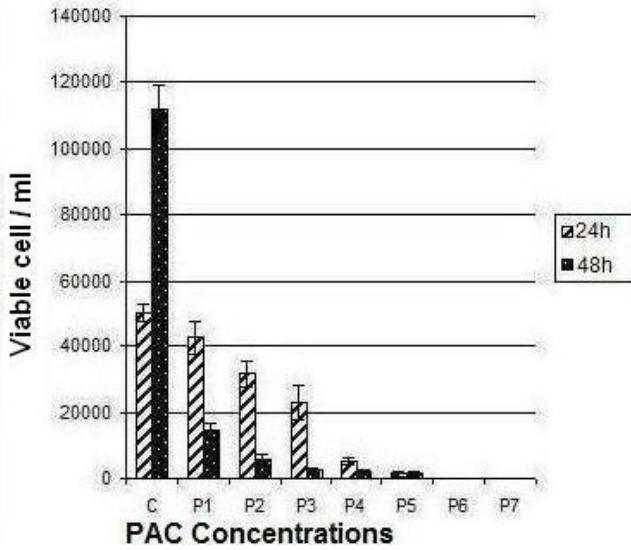


Figure 2. Viable cell number per ml of FM3A cells treated with PAC (P1 = 3 nM, P2 = 7.5 nM, P3 = 15 nM, P4 = 30 nM, P5 = 60 nM, P6 = 120 nM, P7 = 240 nM).

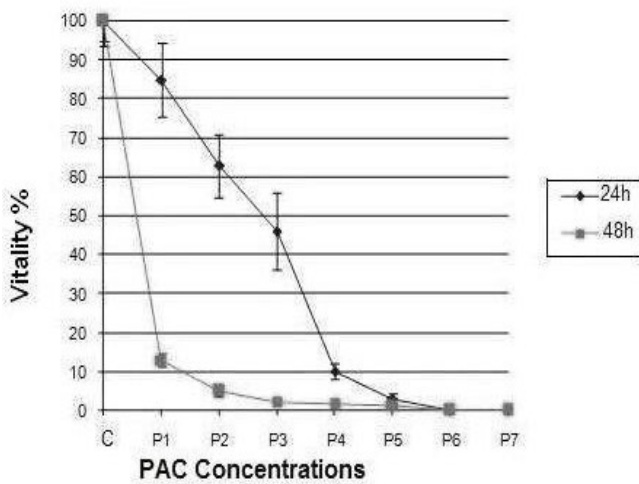


Figure 3. Vitality % values of FM3A cells treated with PAC (P1 = 3 nM, P2 = 7.5 nM, P3 = 15 nM, P4 = 30 nM, P5 = 60 nM, P6 = 120 nM, P7 = 240 nM).

63% for P2 dose, 46% for P3 dose, 10% for P4 dose, 3% for P5 dose, and 0% for P6 and P7. Statistically significant differences between treatment and control group were detected ($p < 0.05$). Vitality % for 48 h were detected as, 12.9% for P1, 4.9% for P2, 2.23% for P3, 1.78% for P4, 1.33% for P5, and 0% for P6 and P7 doses. All the differences between treatments and control group were statistically significant ($p < 0.05$). Dead cells number for 24 and 48 h are shown in Figure 4. We observed that seven doses of PAC and time dependent increasing of dead cell number was consistent with decrease on proliferation rate graph.

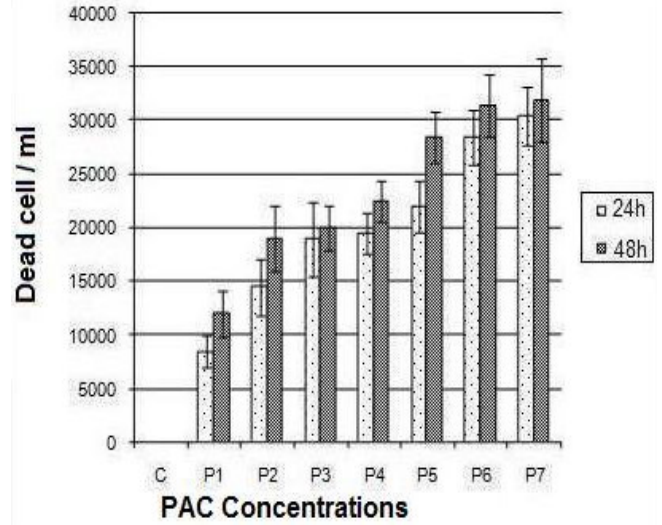


Figure 4. Dead cell number per ml of FM3A cells treated with PAC (P1 = 3 nM, P2 = 7.5 nM, P3 = 15 nM, P4 = 30 nM, P5 = 60 nM, P6 = 120 nM, P7 = 240 nM).

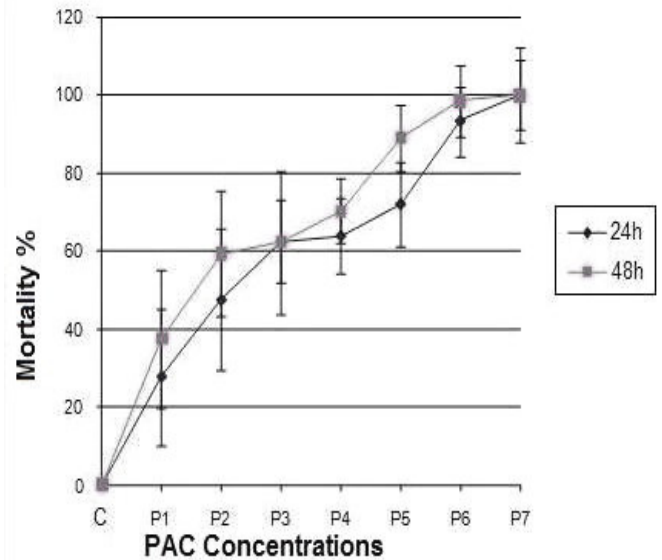


Figure 5. Mortality % values of FM3A cells treated with PAC (P1 = 3 nM, P2 = 7.5 nM, P3 = 15 nM, P4 = 30 nM, P5 = 60 nM, P6 = 120 nM, P7 = 240 nM).

Compared to the most cytotoxic group whose mortality was 100%, mortalities of experiment groups after 24 and 48 h are shown in Figure 5. Therefore, the seven doses of PAC have time and dose dependent increasing cytotoxic effects on FM3A cells. Cytotoxic effects which occurred in our experiments was detected by assessment of decreasing surviving cell numbers (vitality %) and increasing dead cell numbers (mortality %).

WST-1 colorimetric results: Absorbance measurement for 24 and 48 h are shown in Figure 6. Vitality % graph

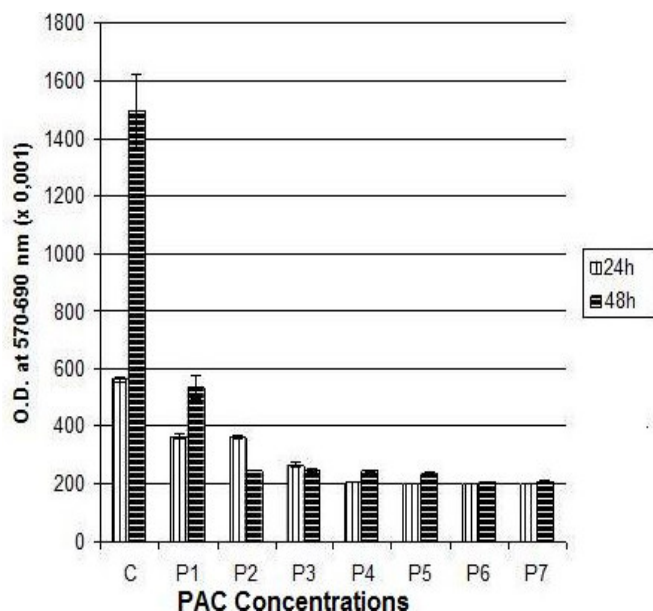


Figure 6. WST-1 results of FM3A cells treated with PAC (P1 = 3 nM, P2 = 7.5 nM, P3 = 15 nM, P4 = 30 nM, P5 = 60 nM, P6 = 120 nM, P7 = 240 nM).

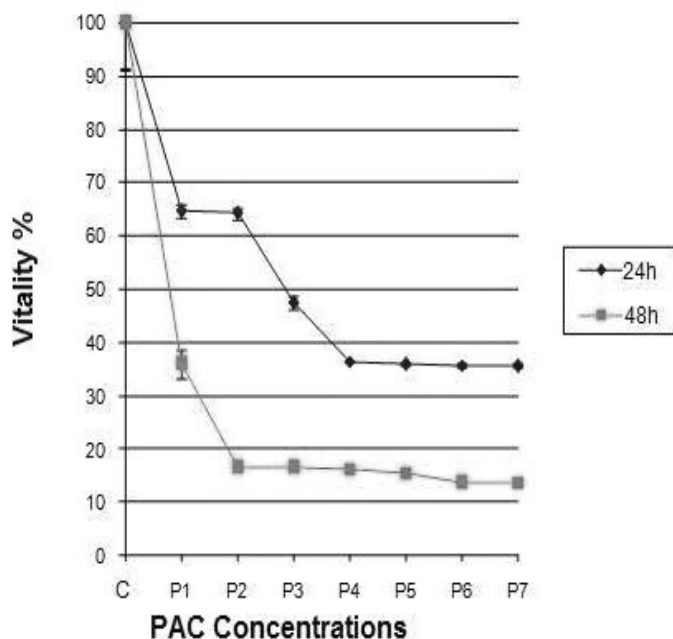


Figure 7. Vitality % values of FM3A cells treated with PAC (P1 = 3 nM, P2 = 7.5 nM, P3 = 15 nM, P4 = 30 nM, P5 = 60 nM, P6 = 120 nM, P7 = 240 nM).

which was determined by absorbance measurement is shown on Figure 7. Compared to control group, vitality % values of experiment groups which were examined for their mitochondrial dehydrogenase enzyme activity after 24 h were determined as 64.7% for P1, 64.3% for P2,

47.4% for P3, 36.5% for P4, 36% for P5, 35.8% for P6 and 35.7% for P7. Vitality % values for 48 h were determined as 35.9% for P1, 16.6% for P2 and P3, 16.4% for P4, 15.7% for P5, 13.7% for P6 and 13.9% for P7. All the differences between treatments and control groups (24 and 48 h treatments) were statistically significant ($p < 0.05$). The results of WST-1 colorimetric method were consistent with results of hemocytometer measurement.

Evaluation of paclitaxel-induced apoptosis in FM3A cells

Morphological methods: Expected apoptotic morphological changes were shrinkage of cell membrane, blebbing of cell membrane, nuclear condensations; thus cell deformation and formations of apoptotic bodies. Afterwards, nucleus breaks into fragments. In our study this apoptotic morphological changes were detected on PAC treated FM3A by Phase-contrast microscope as shown in Figure 8.

Formations of vacuole blebbing, nuclear condensations and apoptotic bodies, which occurred in treated cells, were detected by Giemsa staining (Figure 9), and fluorescent microscopy with DAPI as shown in Figure 10.

Apoptotic index (AI): 24 h after drug treatments, there were no apoptotic cells among 200 cells of control group of FM3A. 200 cells per treatments group were taken and 73% for P1, 85% for P2, 64% for P3, 31% for P4, 24% for P5, 22% for P6 and 17% for P7 were detected as apoptotic. All differences between control and treatments groups were statistically significant (Figure 11) ($p < 0.05$). Apoptotic cell number after 48 h treatments were 124% for P1, 135% for P2, 94% for P3, 52% for P4, 26% for P5, 23% for P6, and 19% for P7 doses. All the differences between treatments and control groups (24 and 48 h treatments) were statistically significant ($p < 0.05$). Compared to the control group which was supposed to have 100% vitality, vitality values of drug treated groups after 24 and 48 h were statistically significant ($p < 0.05$) compared to control (Figure 12). AI values for P2 dose increased for both 24 and 48 h of PAC treatments.

DNA fragmentations: As an indicator of apoptosis, DNA fragmentations was detected by Apopladder ExTM (Takara, Kat. No: MK600) kit on seven different doses of PAC treatment for two different times (24 and 48 h) in FM3A cells. DNA fragmentation results of cancer cells which were treated with various doses of PAC for 24 h are showed in Figure 13. Compared to control group, 24 h after PAC treatments, 200 bp long DNA fragmentations was detected on P2 treated FM3A cells (Figure 13). Also 48 h after PAC treatments, 300 - 350 bp long DNA fragmentations were detected on treated FM3A cells (Figure 14).

General evaluation: We aimed to determine apoptotic and anti-proliferative effects of PAC on FM3A cells, and results showed us that seven different doses of PAC have

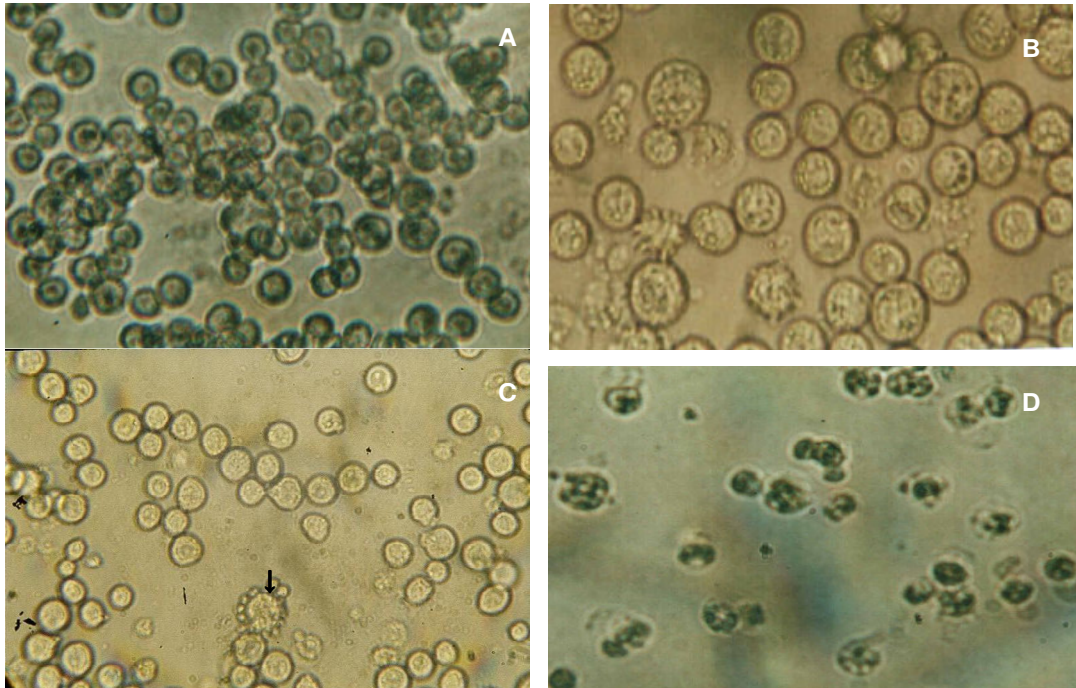


Figure 8. Phase-contrast microscopy (FM3A cells in apoptosis ↑) (x400) **A.** Control. **B** and **C.** Nuclear fragmentations and formations of bleb after P2 treatments (↑) **D.** Secorder necrosis after P7 treatments (↑).

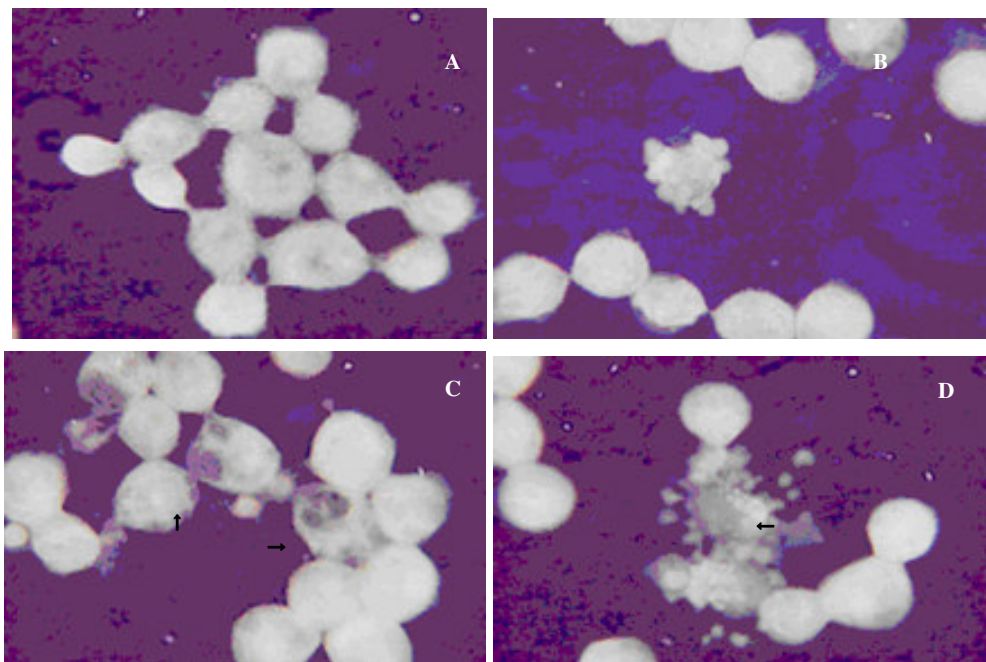


Figure 9. Apoptotic FM3A cells with Giemsa staining after P2 treatments (x100). **A.** Control. **B.** Formations of bleb. **C.** Formations of vacuole. **D.** Nuclear condensations.

have cytotoxic effects on FM3A cells when they are applied for 24 and 48 h. Cytotoxic effects of PAC caused significant proliferation speed decreasing ($p < 0.05$) from

the first treatments group to the last, comparing to control group. Cytotoxic effects which we obtained was because of PAC-induced apoptosis. Apoptosis which occurred on

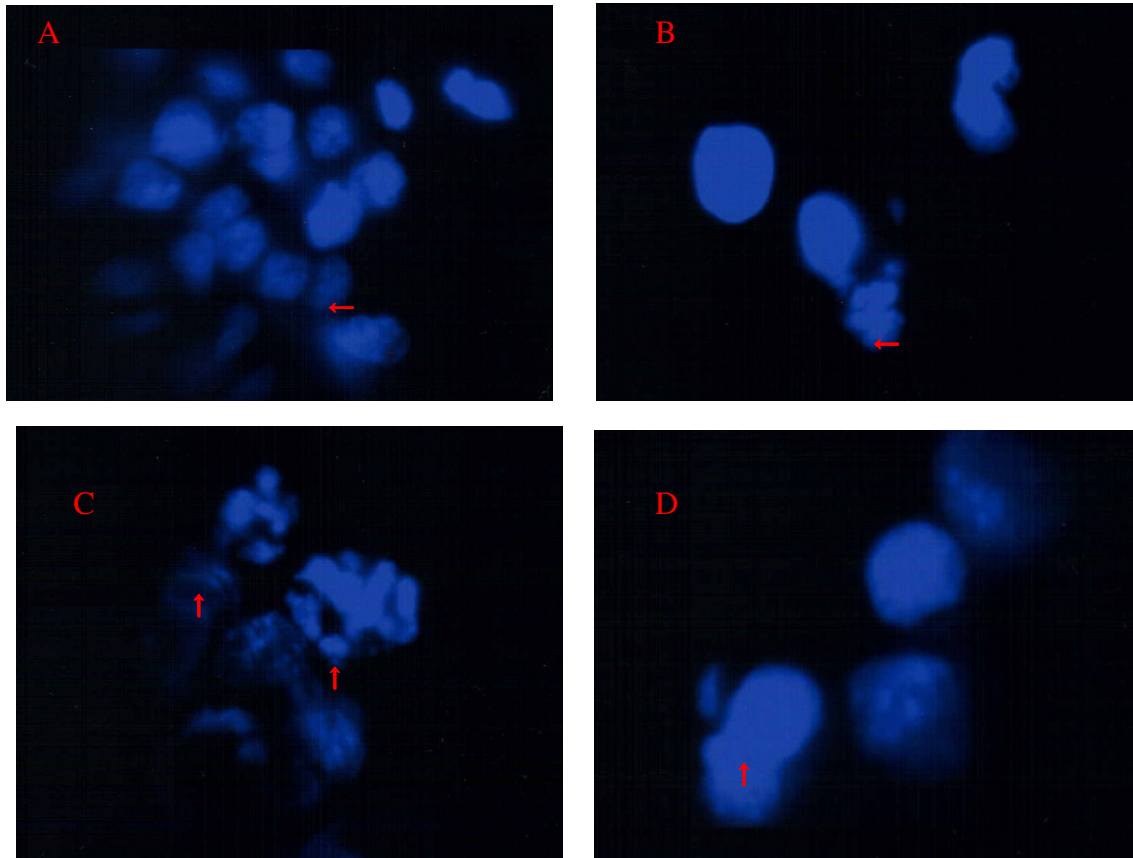


Figure 10. Fluorescence microscopy of P2 treatments with DAPI in FM3A cells (x100). **A.** Control. **B, C** and **D.** Apoptotic cell nucleus.

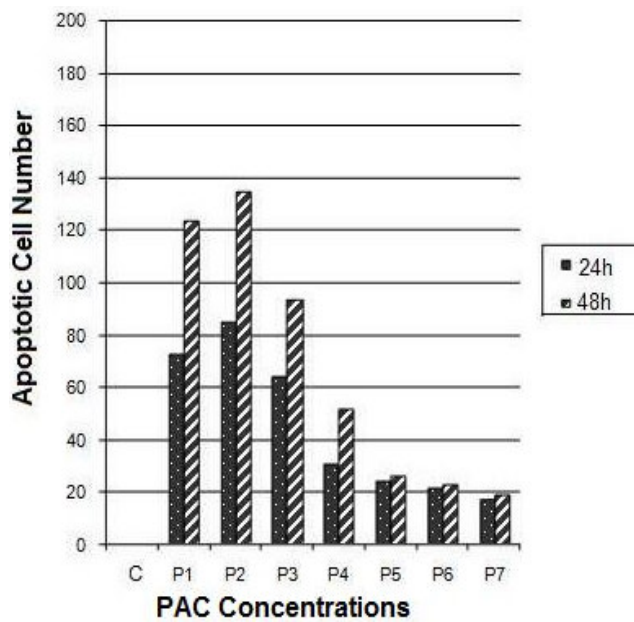


Figure 11. Apoptotic cell number of FM3A cells treated with PAC (P1 = 3 nM, P2 = 7.5 nM, P3 = 15 nM, P4 = 30 nM, P5 = 60 nM, P6 = 120 nM, P7 = 240 nM).

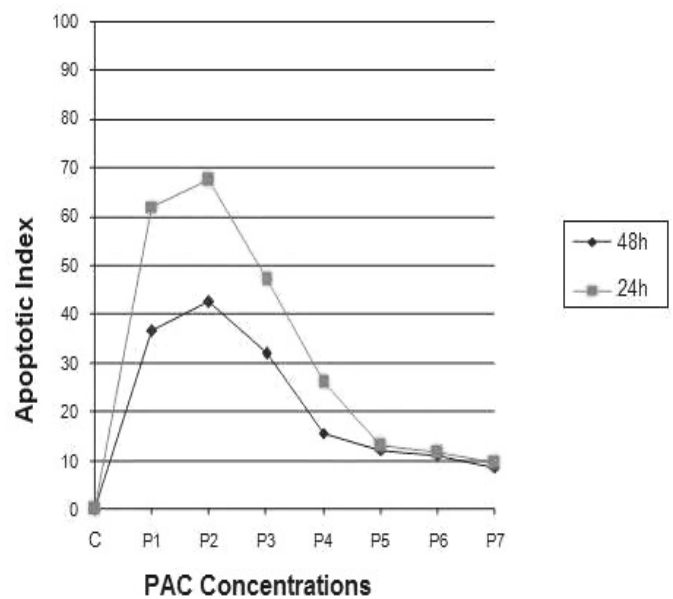


Figure 12. Apoptotic index of FM3A cells treated with PAC (P1 = 3 nM, P2 = 7.5 nM, P3 = 15 nM, P4 = 30 nM, P5 = 60 nM, P6 = 120 nM, P7 = 240 nM).

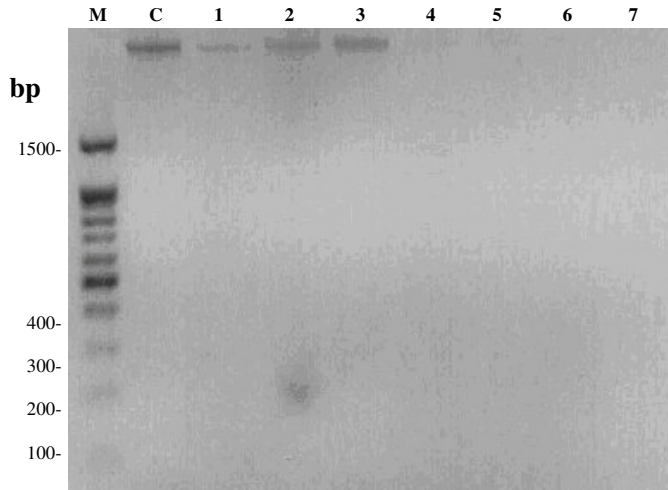


Figure 13. Agarose gel electrophoresis of DNA fragmentations after PAC treatments for 24 h (M. Marker, C. Control, 1. P1, 2. P2, 3. P3, 4. P4, 5. P5, 6. P6, 7. P7).

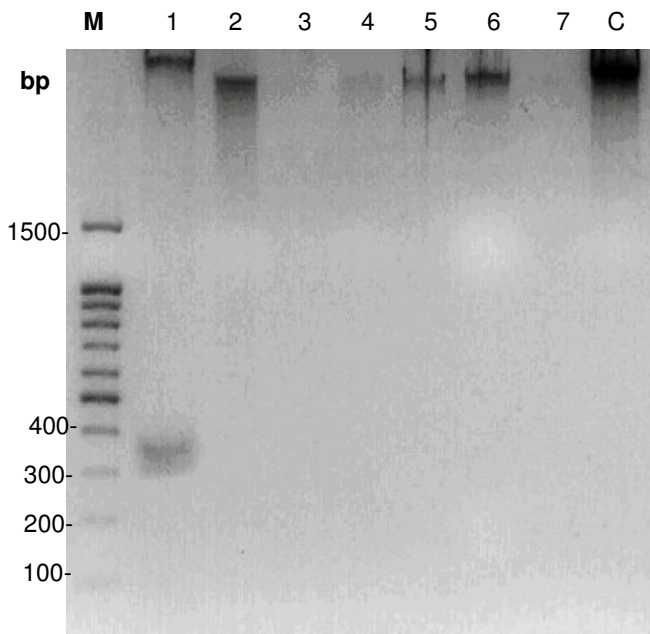


Figure 14. Agarose gel electrophoresis of DNA fragmentations after PAC treatments for 48 h. (M. Marker, C. Control, 1. P2, 2. P1, 3. P6, 4. P5, 5. P4, 6. P3, 7. P7).

PAC treated FM3A cells was supported by morphological imaging, molecular biology methods and also by AI parameters. Among all parameters that we applied, P2 gave the highest apoptotic index values and also it was the only one which had DNA fragmentations on agarose gel electrophoresis. We found that P2 dose is the most effective one for FM3A cells.

DISCUSSION

Cancer is a process in which normal cells gain infinite proliferation ability and drives organism to the death. Unfortunately our knowledge about molecular changes which occurs at cancer development and invasion is insufficient. Observing responses of cancer cells to anti-cancer drugs, and driving them to apoptosis by developing their activities seem to be one of the best ways (Lanni et al., 1997; Sawada et al., 2003). Apoptosis is a selective process which we can see on normal physiological and pathological conditions and also erases the cells which can potentially harm the organism (Bribiesca, 2003; Crowell, 2005). Apoptotic cell is characterized by loss of volume, swelling of plasma membrane, nuclear condensations, aggregation of cromatine, and nucleosomal DNA fragmentations (Arican et al., 2008).

In our study, toxicity increased depending on dose of PAC on the treated FM3A cells. Surviving cells decreased depending on time and dose, while dead cells were increased. Multiple effects of PAC include increasing polymerization and stabilization of microtubules, and blocking cell cycle on G2/M phase. This caused anti-proliferation of tumor cells lines of murin solid tumor and leukeamia, and also caused cell death (apoptosis) (Jordan et al., 1996; Chen et al., 1997; Arican Özcan, 2005a).

Another paper on this subject shows that cytotoxic effects of PAC occurs by suppressing cell proliferation, accumulation on mitosis phase (G2/M blockage) and therefore decreasing on synthesis phase (Arican, 2005b). Microtubules support cells physically and also built intracellular substructure for signal transmitting pathways. Microtubules fill whole cytoplasm and cross whole cell from membrane to nucleus. Previous studies showed that microtubules are related with mechanic components of both apoptosis and cell cycle (Vikhanskaya et al., 1998). Due to PAC's multiple effects on cell cycle and apoptosis, it should not be surprising to observe that it kills cancer cells (Long and Fairchild, 1994; Pulkkinen et al., 1996; Lieu et al., 1997; Wang et al., 2000). PAC kills cancer cells by p53-independent way. It kills p53 mutant cancer cells more effective than wild type p53 containing cancer. Also, PAC acts selective to transformed cells and blocks them on G2/M phase of cell cycle or drives them to apoptosis. On non-transformed cells, it caused reversible G1 blockage (Wang et al., 2000).

PAC-induced apoptosis can also be regulated by bcl-2 subfamily members. Bcl-2 family contains both death inducers (Bax, Bak, Bad, Bcl-XS; proapoptotics) and death suppressors (Bcl-2, Bcl-XL; antiapoptotics) (Wang et al., 2000). It was shown by Liu and Stein (1997) and Wang et al. (2000) that PAC caused down-regulation of Bcl-XL expression and by Liu and Stein (1997), Jones et al. (1998) and Wang et al. (2000) that it caused up-regulation of Bax and Bak expression. It was shown that PAC treatments start phosphorylation of bcl-2 and also it was reported by Blagosklonny et al. (1996, 1997), Haldar

et al. (1998) and Wang et al. (2000) that Raf-1 is essential for this phosphorylation. The latest studies proved that bcl-2 phosphorylation after PAC treatments occurs only at cells which were blocked on G2/M phase (Haldar et al., 1998; Scatena et al., 1998; Wang et al., 2000). PAC-induced apoptosis is related with activation of p34cdc2 (Ibrado et al., 1998; Wang et al., 2000), cdc-like kinase (Scatena et al., 1998; Wang et al., 1998) and other cyclin-dependent kinases (CDKs) (Ponnathpur et al., 1995; Meikrantz and Schlegel, 1996; Wang et al., 2000). Recent researches indicate that activation of p34cdc2 is related to apoptosis and CDKs are among terminal effectors of apoptotic process (Wang et al., 2000). The question of activation of p34cdc2 being reason (Yu et al., 1998) or result (Ling et al., 1998) of mitotic stoppage is not answered completely yet (Wang et al., 2000). Alternatively, activation of p34cdc2 and mitotic stoppage can be two possible results of dynamic microtubules suppression (Ling et al., 1998; Wang et al., 2000).

Mitotic stoppage is related to apoptosis on PAC-treated cells. PAC-induced apoptosis can be observed directly right after a mitotic stoppage or after entering G1-like multi nucleus including abnormal conditions (Wang et al., 2000). Mitotic spindle checkpoint is a signal transmitting pathway which observes correct connections between chromosomes and mitotic spindle, and continues until cell cycle blocking results. It is connected with kinetochore-related receptor. Various mammalian gene products such as MAD2, BUB1, BUB3, PP2A and MAPK are described to function in spindle accumulation checkpoint (Wang et al., 2000). Apoptosis which is characterized by specific changes on cell surface and nuclear morphology is a morphological and biochemical process that drives cell to death. Internucleosomal level DNA fragmentations can be observed in apoptotic cells (Collins et al., 1997).

In our experiment, cytotoxic effects of PAC is related to cell death using growth rate parameter. To understand that if this cell death occurs by apoptosis or not, we used DAPI staining and searched by fluorescence microscope. We found that P2 is the most effective dose. We detected that as the dose increased, the number of apoptotic cells decreased. By the way, we have to search for more parameters to understand the way which cells are heading when they were treated with higher doses than P2. When we looked for morphological criterion of PAC-induced apoptosis we found the same P2 dose as the most effective for cell shrinkage, blebbing of cell membrane, formations of apoptotic bodies, nuclear condensations, fragmentations and seconder necrosis (Figures 8 - 10).

To support apoptotic effects of PAC in this study we detected DNA fragmentations which is one of the main properties of apoptosis. As a support to this finding, agarose gel electrophoresis results confirmed that DNA fragmentations occurs at P2 dose. We could not see DNA fragmentations on other doses for this treatments

periods except P2 dose, but it does not mean that DNA fragmentations does not occurs at the other doses (Figure 13 - 14). The result that we found support results of the other researches which points apoptotic and anti-proliferative effects of PAC on tumor cells.

Criteria of growth rate inhibition, AI increasing, characteristic changes of apoptosis and DNA fragmentations are limited to explain mechanism of cytotoxic effects of PAC. However, time and dose dependent increase of cytotoxicity, and its apoptotic pathways are consistent with previous studies. Especially, P2 dose (7.5 nM) of PAC sensitivity of FM3A cells, is the major result of our study. Future studies which takes this best dose as reference will provide critical assessment of clinical usage of PAC.

ACKNOWLEDGMENT

This work was supported by the Research Fund of The University of Istanbul. Project no: T-593/17032005

REFERENCES

- Arican Özcan G (2005a). Evaluation of chemoprotective effects of amifostine and cysteamine in cell cultures treated with using growth rate parameter. *Biologia*. 60: 325-330.
- Arican Özcan G (2005b). Cytoprotective effects of amifostine and cysteamine on cultured normal and tumor cells treated with paclitaxel in terms of mitotic index and 3H-thymidine labeling index. *Cancer Chemother. Pharmacol.* 56: 221-229.
- Arican Özcan G, Serbes U, Arican E (2008). Evaluation of the cytotoxicity between epirubicin and daunorubicin in HeLa cell cultures. *Afr. J Biotechnol.* 7(6): 706-711.
- Blagosklonny MV, Schulte T, Nguyen P, Trepel J, Neckers LM (1996). Taxol-induced apoptosis and phosphorylation of bcl-2 protein involves c-Raf-1 and represents a novel c-Raf-1 signal transduction pathway. *Cancer Res.* 56: 1851-854.
- Blagosklonny MV, Giannakakou P, el-Deiry WS, Kingston DG, Higgs PI, Neckers L (1997). Raf-1/bcl-2 phosphorylation: a step from microtubule damage to cell death. *Cancer Res.* 57: 130-135.
- Bribiesca LB (2003). The pathways of apoptosis: one led to Stockholm, the other led to home. *Arch. Med. Res.* 34: 1-2.
- Chen CT, Au JLS, Gan Y, Wientjes MG (1997). Differential time dependency of antiproliferative and apoptotic effects of taxol in human prostate tumors. *Urol Oncol.* 3: 11-17.
- Collins JA, Schandl CA, Young KK, Vesely J, Willingham MC (1997). Major DNA fragmentation is a late event in apoptosis. *J. Histochem. Cytochem.* 45(7): 923-934.
- Crowell JA (2005). The chemopreventive agent development research program in the Division of Cancer Prevention of the US National Cancer Institute: An overview. *Eur. J. Cancer.* 41(13): 1889-1910.
- Haldar S, Jena N, Croce CM (1998). Inactivation of Bcl-2 by phosphorylation: a step from microtubule damage to cell death. *Proc. Natl. Acad. Sci. USA.* 57: 130-135.
- Hu W, Kavanagh J (2003). Anticancer therapy targeting the apoptotic pathway. *Lancet Oncol.* 4: 721-729.
- Ibrado AM, Kim CN, Bhalla K (1998). Temporal relationship of CDK1 activation and mitotic arrest to cytosolic accumulation of cytochrome C and caspase-3 activity during Taxol-induced apoptosis of human AML HL-60 cells. *Leukemia.* 12: 1930-1936.
- Jones NA, Turner J, McIlwrath AJ, Brown R, Dive C (1998). Cisplatin- and paclitaxel-induced apoptosis of ovarian carcinoma cells and the relationship between bax and bak up-regulation and the functional status of p53. *Mol. Pharmacol.* 53: 819-826.

- Jordan MA, Wendell K, Gardiner S, Derry WB, Copp H, Wilson L (1996). Mitotic block induced in HeLa cells by low concentrations of paclitaxel (Taxol) results in abnormal mitotic exit and apoptotic cell death. *Cancer Res.* 56: 816-825.
- Kim R, Tanabe K, Uchida Y, Emi M, Inoue H, Toge T (2002). Current status of the molecular mechanisms of anticancer drug-induced apoptosis. *Cancer Chemother. Pharmacol.* 50: 343-352.
- Lanni JS, Lowe SW, Licitra EJ, Liu JO, Jacks T (1997). p53-independent apoptosis induced by paclitaxel through an indirect mechanism. *Proc. Natl. Acad. Sci. USA.* 94: 9679-9683.
- Lieu CH, Chang YN, Lai YK (1997). Dual cytotoxic mechanisms of submicromolar Taxol on human leukemia HL-60 cells. *Biochem Pharmacol.* 53: 1587-1596.
- Ling YH, Tornos C, Perez-Soler R (1998). Phosphorylation of bcl-2 is a marker of M phase events and not a determinant of apoptosis. *J. Biol. Chem.* 273: 18984-18991.
- Liu QY, Stein CA (1997). Taxol and estramustine-induced modulation of human prostate cancer cell apoptosis via alteration in bcl-xL and bax expression. *Clin Cancer Res.* 3: 2039-2046.
- Lockshin RA, Zakeri Z (2004). Apoptosis, autophagy, and more. *Int. J. Biochem. Cell Biol.* 36: 2405-2419.
- Long BH, Fairchild CR (1994). Paclitaxel inhibits progression of mitotic cells to G1 phase by interference with spindle formation without affecting other microtubule functions during anaphase and telephase. *Cancer Res.* 54: 4355-4361.
- Mastropaolo D, Camerman A, Luo Y, Brayer G, Camerman N (1995). Crystal and molecular structure of paclitaxel (taxol). *Proc. Natl. Acad. Sci. USA* 92: 6920-6924.
- Meikrantz W, Schlegel R (1996). Suppression of apoptosis by dominant negative mutants of cyclin-dependent protein kinases. *J. Biol. Chem.* 271: 10205-10209.
- Moos PJ, Fitzpatrick FA (1998). Taxane-mediated gene induction is independent of microtubule stabilization: induction of transcription regulators and enzymes that modulate inflammation and apoptosis. *Proc Natl Acad Sci USA.* 95: 3896-390.
- Ponnathpur V, Ibrado AM, Reed JC, Ray S, Huang Y, Self S (1995). Effects of modulators of protein kinases on Taxol-induced apoptosis of human leukemic cells possessing disparate levels of p26BCL-2 protein. *Clin. Cancer Res.* 1: 1399-1406.
- Pulkkinen JO, Elomaa L, Joensuu H, Martikainen P, Servomaa K, Grenman R (1996). Paclitaxel-induced apoptotic changes followed by time-lapse video microscopy in cell lines established from head and neck cancer. *J. Cancer Res. Clin. Oncol.* 122: 214-218.
- Sawada S, Mese H, Sasaki A, Yoshioka N, Matsumura T (2003). Combination chemotherapy of paclitaxel and cisplatin induces apoptosis with bcl-2 phosphorylation in ac cisplatin-resistant human epidermoid carcinoma cell line. *Cancer Chemother. Pharmacol.* 51: 505-511.
- Scatena CD, Stewart ZA, Mays D, Tang LJ, Keefer CJ, Leach SD (1998). Mitotic phosphorylation of Bcl-2 during normal cell cycle progression and Taxol-induced growth arrest. *J. Biol. Chem.* 273: 30777-30784.
- Vikhanskaya F, Vignati S, Beccaglia P, Ottoboni C, Russo P, D'incalci M (1998). Inactivation of p53 in a human ovarian cancer cell line increases the sensitivity to paclitaxel by inducing G2/M arrest and apoptosis. *Exp. Cell Res.* 241: 96-101.
- Wang TH, Wang HS, Ichojo H, Giannakakou P, Foster JS, Fojo T (1998). Microtubule-interfering agents activate c-Jun-N-terminal kinase/stress-activated protein kinase through both Ras and apoptosis signal-regulating kinase pathways. *J. Biol. Chem.* 273: 4928-4936.
- Wang TH, Wang HS, Soong YK (2000). Paclitaxel-induced cell death. *Cancer* 88(11): 2619-2628.
- Yi-ting J, Xue-xiang Y, Yi-hong H, Qiang Z, Hong-ying W, Yong-hua X (2008). aPKC Inhibitors Might be the Sensitizer of Chemotherapy and Adoptive Immunotherapy in the Treatment of hASIPa-Overexpressed Breast Cancer. *Oncol. Res.* 17: 59-68.
- Yu D, Jing T, Liu B, Yao J, Tan M, McDonnell TJ (1998). Overexpression of ErbB2 blocks Taxol-induced apoptosis by upregulation of p21Cip1, which inhibits p34Cdc2 kinase. *Mol Cell.* 2: 581-591.